DOI: 10.21062/mft.2025.071 http://www.journalmt.com

Experimental Measurement of Defects Propagation for a Passenger Car Tire Casing under Dynamic Loading

Ján Vavro jr. (0009-0009-6787-9041)[1], Ján Vavro (0009-0001-3704-4934)[1], Lukáš Klimek (0009-0000-9525-414X)[1], Miloš Taraba (0009-0000-2006-8350)[1], Tomasz Domański (0000-0002-5375-5402)[2], Zbigniew Saternus (0000-0002-3837-1072)[2], Petra Dubcová (0000-0003-3450-3290)[1],
[1]Faculty of Industrial Technologies in Púchov, Alexander Dubček University of Trenčín, I. Krasku 491/30, 020 01 Púchov, Slovakia. E-mail: jan.vavro.jr @tnuni.sk, jan.vavro@tnuni.sk, pavol.cernava@tnuni.sk, lukas.klimek@tnuni.sk, milos.taraba@tnuni.sk, petra.dubcova@tnuni.sk,
[2]Faculty of Mechanical Engineering, Czestochowa University of Technology, Dabrowskiego 69, 42-201 Czestochowa, Poland. E-mail: tomasz.domanski@pcz.pl, zbigniew.saternus@pcz.pl,

The given paper deals with the defects propagation in car tires for passenger vehicles under dynamic loading. The occurrence of defects has the significant influence on the lifetime and quality of the tire, especially during its operation as a part of the vehicle. The given defects are closely connected with a safety in road traffic. The aim of the study was to carry out a non-destructive analysis of the car tire for the purpose to analyze the defects propagation as well as to introduce the defects classification and their location along with the whole course of rupture as a result of increasing speed, loading and the number of hours or kilometers driven. During the analysis, we used a non-destructive method for detecting defects using a non-destructive analyzer that works on the principle of shearography. The experimental measurement was carried out for 12 car tires. The measurement results are displayed from the non-destructive analyzer in the form of protocols from measurement and video display. The evaluation of the results of the measurement for the propagation of defects is displayed graphically. In relation to the tire casing, the analysis of the defects propagation can help design engineers to solve critical issues by choosing the right material, modifying dimensions of individual components or even by redesigning the overall construction of the tire casing and thus to increase the safety from the aspect of vehicle operation.

Keywords: Measurement, Pressure, Dynamic loading, Non-destructive method, Shearography

1 Introduction

A serious attention is paid to tire testing during the time of tire production. The reason for testing tires is to guarantee their high reliability and durability in road traffic. Under the laboratory conditions, the tires are tested for their various static and dynamic properties, such as weight, hardness, dimensions, and even whether they can withstand the predetermined speed, loading and inflation. The lifetime of tire is monitored in terms of operating conditions as well as tire defects in relation to fatigue, speed (acceleration) or exploitation tests. Nowadays, remaining requests in industry for safety, lifetime and operating safety lead to usage of non-contact material and products diagnostics. In present, there are systems, which are using geometric and physical optic principles. Their sensitivity is in limit of light wave-length in visible area. These systems are characterized by high measuring accuracy, operation simplicity and possibility of experiment automation. Higher mentioned facts are also confirmed with subsequent review of used methods as it is mentioned in bibliography. In the literature [1], the various methods of shearography and holography and their use in tire testing are described. Moreover, the principles of shearography and its application in non-destructive testing of casings are also described in work [2]. In 1998, a patented measuring method of testing rubber specimens at dynamic behavior was published in Rubber World magazine [3]. New optic sensor and its application are described by Doege in work [4]. This new optic technology was developed for non-contact recognition and record of material creep. Sensor was able to recognize designated surface in the point. Material creep measurement can be used for deformation determination. Image of 3D objects is obtained by utilization of co-ordinates measuring through PC for automatic initialization of operating place. Before measuring process, the measuring system must be calibrated and adjusted correctly to be able to obtain correct results [5]. Non-contact measuring systems have many advantages and they can be used at higher impact speeds. In 2002, Degreick introduced [6] relatively simple optic technique for recording deviation (deflection) history from which the speed and force impact history can be defined. Technique is based on relative deviation (deflection) of two grids and can be used for speed measuring

from a few m/s to 200 m/s. In work [7], the optical measuring system based on trigonometric measuring technique is proposed. The sensor is combined from two CCD cameras and line laser. This system can measure 3D object profile in cross-section, compared with approximated profile. Aramis represents a commercial measuring system that can be used for experimental study of non-contact measuring of transparent synthetic surfaces, pressure balloons, using stereo-correlation method, where the images are obtained by two CCD cameras [8]. This system is successfully used also in rubber industry. Holographic interferometry is used for micro-thermal deformation measuring. Calibration apparatus tests are used for measuring general and local deformations [9]. Method of interferometry is based on interference principle of two coherent waves in given area and interference images valuation. Pointed interferometry is new measuring technique called also as pointed interferometry of temporal progression [10]. Method principle is based on capturing of temporary created points at surface, coherent with surface deformation. CCD cameras are also widely used in microscopy [11]. Testing machine, which enables observing of dynamic tires behavior by dynamic tests under the operating conditions, is described by author in work [12]. Experimental results are comparable with simulation results. The latest equipment of LMI company enables non-contact testing for tire casings. Laser lights tire desired part during its rotation and reflected light signal is processed through CCD sensor. This image is evaluated with PC, which is able to detect any tire casing deformation. From individual images, PC is able to compose the whole surface of tire casing [13].

2 Construction (structure) of the tire casing

It is necessary to have knowledge relating to construction of the tire casing because only this is the correct way for specification of areas where the defects are initiated and moreover, it is also much easier to specify the distribution of the mentioned separations, representing the defects. The construction (structure) of tire casing [14] consists of:

- Tread – it is important part of tire casing, because it is in the close or direct contact with the road surface. It is made of blend which has good adhesive properties and high wear resistance;
- Buffer linings – it absorbs circumferential stresses as well as side forces and it absorbs also impacts which occur during the contact with road. It consists of individual layers of rubberized cord while the given layers are laid in a criss-cross formation;
- Cord carcass of casing – it is the basic and supporting part which comprise of one or several linings from rubberized cord and they are laid around the bead plies;
- Filling linings – they are the shaped rubber profiles and they are used for better and smoother mutual junction of individual construction parts relating to tire casing;
- Bead bundle – it reduces deformation in the area where there is the end of cord carcass and protection of bead;
- Sidewall – it protect side part against damage and weather conditions. It is made of blend which is resistant to flex cracking and cracking in common;
- Inner skim rubber – it is rubber lining which can be found on the internal side of tire casing. It is used for protection of cord carcass and in the case of tubeless tire casings, it avoid diffusion of air into the cord carcass of casing;
- Bead reinforcement – it can be fabric as well as steel;
- Bead plies – they consist of steel wires or strips which have high strength. They provide smooth and safe anchoring of cord carcass linings as well as attachment of tire casing to wheel rim.

Fig. 1 represents the given parts mentioned hereinbefore.

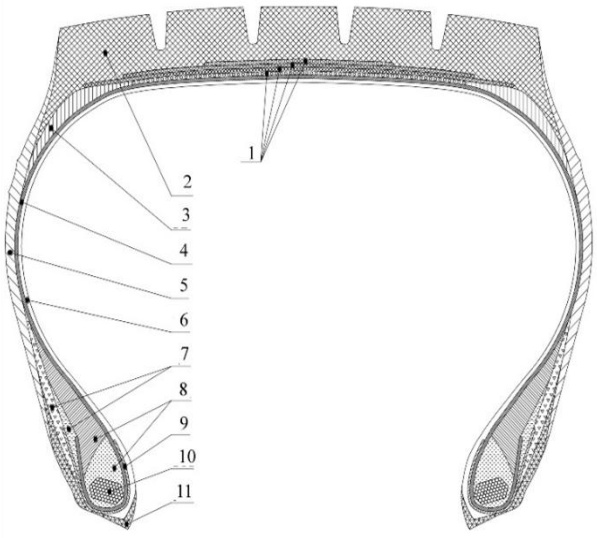

Fig. 1 *The construction (structure) of tire casing: 1- Buffer lining, 2- Tread, 3- Shoulder filler, 4- Cord carcass of casing, 5- Sidewall, 6- Inner skim rubber, 7- Filling linings, 8-Core, 9- Bead reinforcement, 10- Bead plies, 11-Rim strip*

ISSN 1213–2489
e-ISSN 2787–9402

To be suitable for the given purpose, the rubber has to exhibit such properties as good elasticity, strength, resistance to ozone aging, wear resistance and so forth [15]. The tire as a whole has to meet basic criteria, including safety, high durability and comfort properties. As a tire is made up of basic parts, such as carcass, bead bundle, sidewall, and others, each of these parts needs a different type of rubber to be used. The carcass has to exhibit load-bearing properties mainly, so it has to be strong and have a good rubber cord adhesion. The sidewall rubber has to be flexible and resistant to breaking. The tread rubber is expected to be hard and abrasion resistant.

3 Process of measurement by help of non-destructive analyser

The distribution of defects (separations) was investigated with non-destructive analyzer see (Fig. 3) and with help of special drum testing device (IGTT 25 kN – C), where the diameter of drum was 1707 mm (Fig. 2).

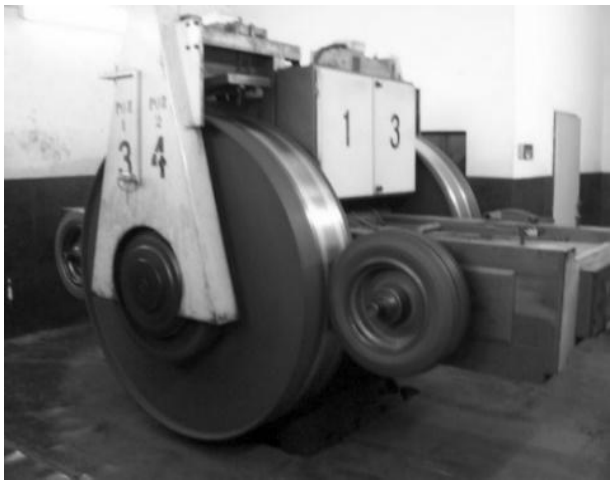

Fig. 2 *The drum testing device*

Fig. 3 *The non-destructive analyser*

Non-destructive analyzer enables us to recognize the tire structure defects quickly and easily – it is connected with closed separations (Fig. 4), the propagation of which is going to be observed by the dynamic test. For the tire impurity searching and the tire control, the charge-coupled device, which uses simple cycle scanning, is utilized as one of the integral and important parts and it can be seen in the Fig. 5.

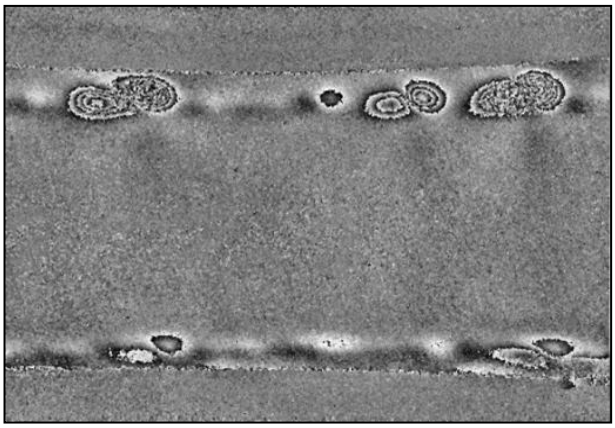

Fig. 4 *The defect – monitor display*

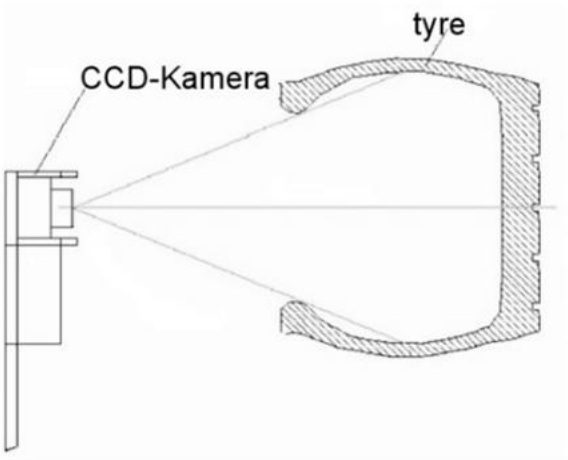

Fig. 5 *T The testing process with the simple cycle*

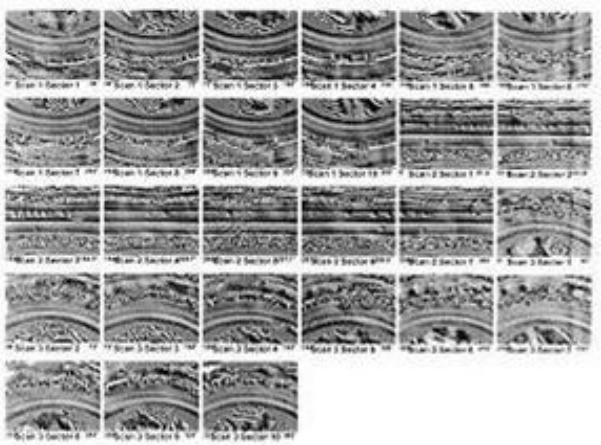

Fig. 6 *The protocol from measurement – phase images from non-destructive testing analyzer*

indexed on http://www.webofscience.com and http://www.scopus.com

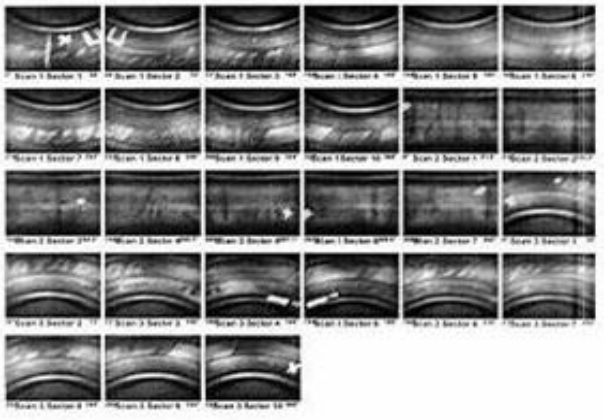

Fig. 7 *The protocol from measurement – video shot from non-destructive testing analyzer*

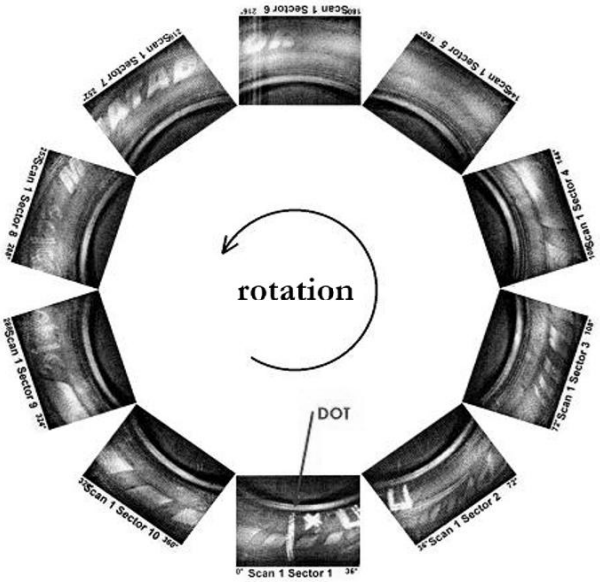

Fig. 8 *The sidewall image for a tire casing from the serial side after the serial diagnostic – arranged into the circle*

Using the non-destructive analyzer as a testing device, the result of the testing process can be obtained in the form of protocol (record) which is based on ITTView program, while the given protocol can be displayed and printed as a phase images (Figure 6), as a video shot (Fig. 7) as well as the specific number of scans arranged into the circle (Fig. 8).

4 Effect of vacuum on the display of separation using a non-destructive analyzer

In order to detect even small local defects inside the casing, it is necessary to fix the camera to non-destructive analyzer as well as to find the correct or the most appropriate position of the given camera. Moreover, it is also important to select the optimum vacuum in the chamber [15-17]. For different casing sizes, different camera positions are required, depending on the casing diameter and the height of the casing profile. Considering the size of the casing dimensions and the height of the casing profile, a single cycle or multiple cycles are then used in order to display either the entire casing area or the area, which is under the investigation (e.g.: crown, sidewall of the casing). For the ITT-1 non-destructive analyzer, the vacuum can be set from 0 to 10 kPa. The camera placement from the horizontal position is 40 mm and the vertical position is 500 mm while camera angle is18°. The tire casing was divided into the eight sectors due to better observation and subsequent analysis. The effect of vacuum setting in the chamber on the error display can be clearly seen in Figures from 9 to 12. For comparison, only two sectors, sectors 4 and 8, were selected out of eight. The best visible defects or separations are at vacuum values from 8 to 10 kPa. When monitoring the casing, vacuum values from 9 to 10 kPa are harder to keep within the allowable tolerance in the chamber of the non-destructive analyzer and thus the scanning time of casing is also increased. Therefore, vacuum values from 4 to 8 kPa are the most suitable and effective for tire testing. These values can be considered as optimum values for the whole range of dimensions examined, using the non-destructive analyzer. For the measurements, the predetermined values of vacuum were 40 mbar and 50 mbar that is 4 kPa and 5 kPa, respectively.

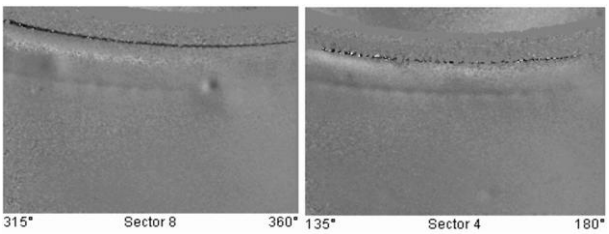

Fig. 9 *The investigation of tire casing in vacuum – 10 mbar = 1 kPa*

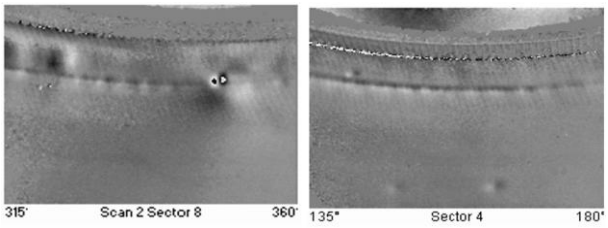

Fig. 10 *The investigation of tire casing in vacuum – 40 mbar = 4 kPa*

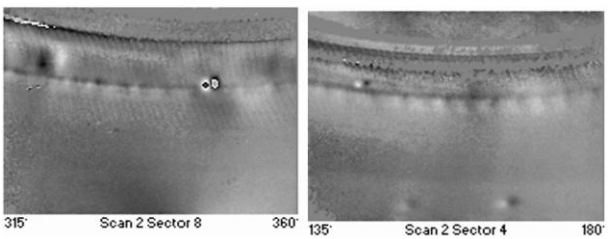

Fig. 11 *The investigation of tire casing in vacuum – 50 mbar = 5 kPa*

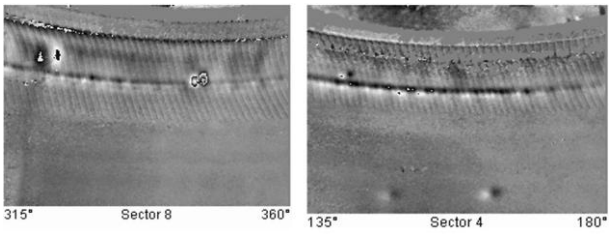

Fig. 12 *The investigation of tire casing in vacuum – 100 mbar = 10 kPa*

5 Results of defects measurement for the tire casing – obtained with the laser interferometry

On the basis of the obtained knowledge from the tire casings analyses, some of repeating defects or separations for tire casing were identified and a subsequently, the list of defects was created to the displayed results from the ITT-1 non-destructive analyser. The images on the left side show the casing defects obtained from the non-destructive analysis and the images on the right side show the photographs of the casing after the cut sections were carried out for a given defect location. The basic types of separations in the site of shoulder and crown area of tire casing can be seen in Figures from 13 to 26.

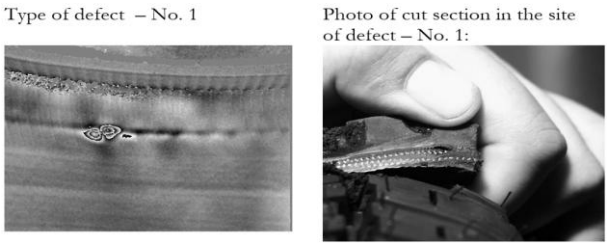

Fig. 13 *The local defect in the site where the second buffer lining end*

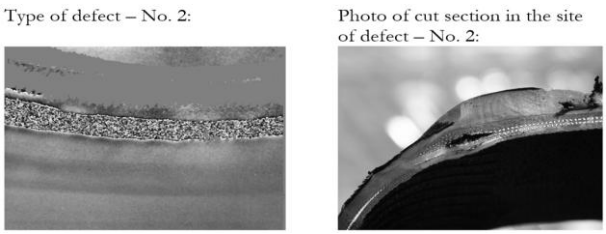

Fig. 14 *The longitudinal continuous defect in the shoulder between the first and second buffer lining*

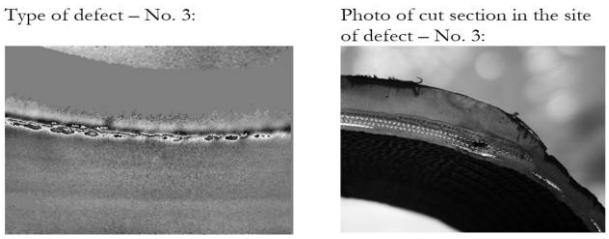

Fig. 15 *The longitudinal chain defect in the shoulder between the first and the second buffer lining*

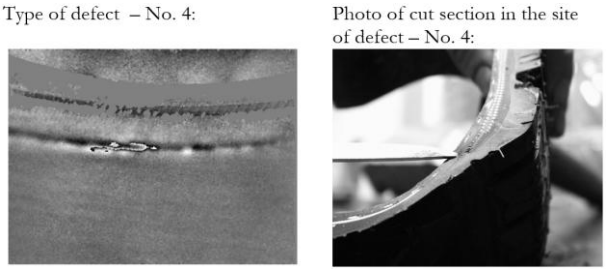

Fig. 16 *The local defect in the shoulder where the first buffer lining ends*

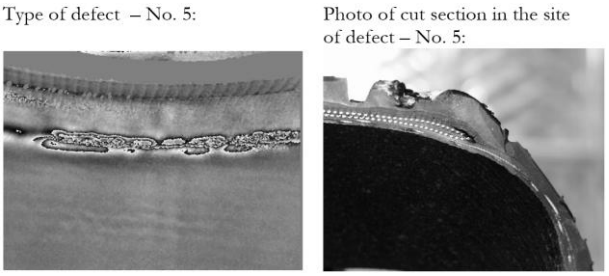

Fig. 17 *The longitudinal defect in the shoulder where the first and the second buffer linings end and its propagation to the crown*

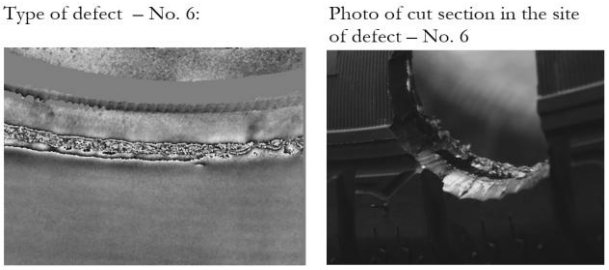

Fig. 18 *The longitudinal defect in the shoulder and its propagation to the sidewall directions*

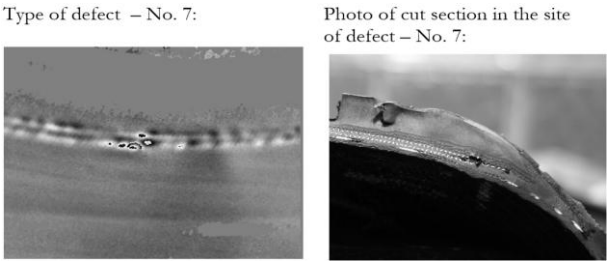

Fig. 19 *The local defect in the shoulder in the site where the second buffer lining ends*

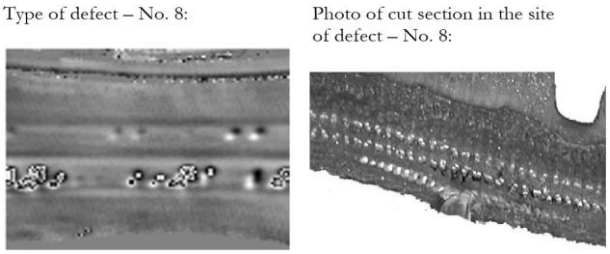

Fig. 20 *The local defect in the crown between the first buffer lining and the cord carcass*

The basic types of defects in the sidewall area and bead area of tyre casing.

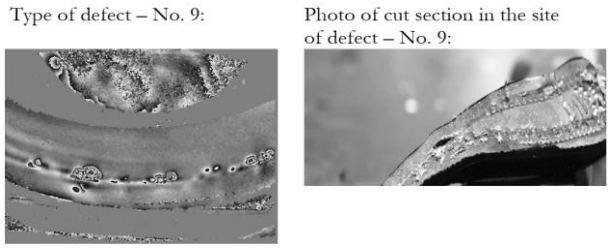

Fig. 21 *The local defect in the sidewall between the end of carcass lining and bead bundle*

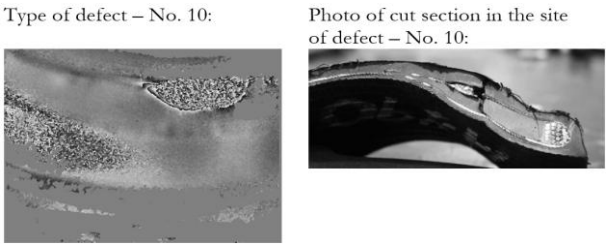

Fig. 22 *The local defect in the sidewall – burst bead rubber and bead bundle – defect between the carcass end of lining and bead bundle*

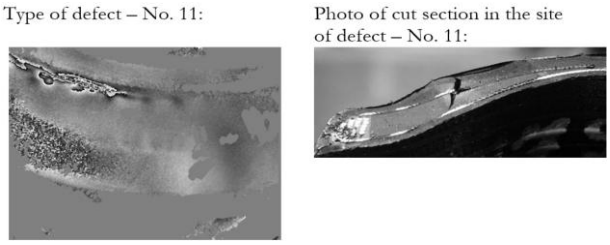

Fig. 23 *The local defect of the tire casing - burst bead rubber and bead bundle*

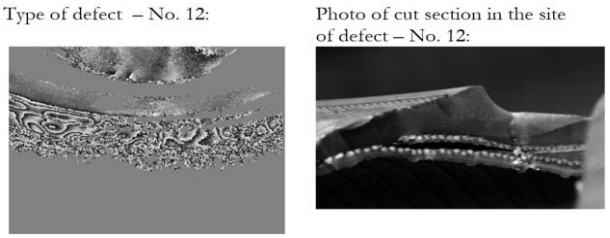

Fig. 24 *The longitudinal defect in the sidewall of the tire casing – it is in the site where the carcass lining is bent*

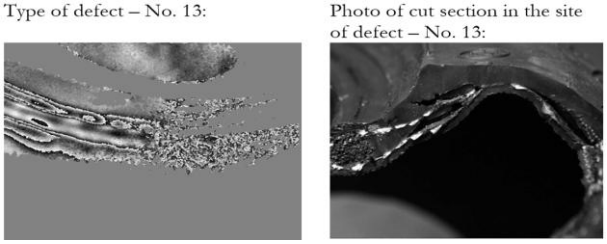

Fig. 25 *The longitudinal defect in the shoulder and sidewall of the tire casing between the bent carcass lining and filling linings of bead bundle*

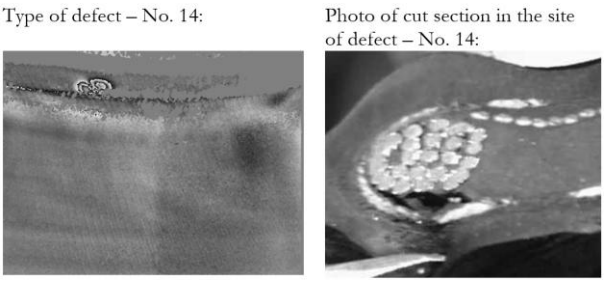

Fig. 26 *The local defect in the bead area between bead plies and bent - burst bead rubber and bead bundle carcass lining*

6 Influence of material and construction (structural) changes in the shoulder zone on the propagation of defects in tire casing

In order to investigate the effect of material and construction changes on the defect propagation in the tire, the investigation process was performed for twelve pieces of tire casings with dimensional designation of 12 225/75 R 16 C while the tread profile was the same in the case of all tested pieces of tire casing. The individual tires were designated as Variants from 1 to 12 (V001-V012). For these variants, two types of blends as well as different construction changes in the shoulder zone were used and one of the variants was a conventional mass production tire [18-22]. The tire casings were tested with the 75 kN -G drum testing machine which was provided by IGTT company. Moreover, they were tested with the ITT-1 non-destructive analyzer from SDS company. An overview of the different tire variants is given in Tab. 1.

The process for the investigation of defect propagation of errors was based on the following steps:

- Carrying out a non-destructive analysis for new tire casings,
- Dynamic fatigue testing of casings, using drum testing machines,
- Continuous testing or control testing of tire casings, using non-destructive analyzer,
- Destructive analysis of tire casings – cut sections,
- Evaluation.

All tire casings were subjected to fatigue testing process under the following conditions:

- Testing loading: 22 760 N
- Testing compression (inflation): 575 kPa
- Testing speed: 40 km/h
- Time Interval of Duration: 20 h
- Conditioning or setting time including analyzer testing process: approx. 4 h

Tab. 1 *Overview of individual tire variants*

Number of tire casing	Number of Variant	Material	Construction
1	V001	SC - A, EC – A, blend A	BL1 – A, BL 2 – B
2	V002	SC - A, EC – A, blend A	BL1 – A, BL 2 – B, BL3 – C
3	V003	SC - A, EC – A, blend A	BL1 – A, BL 2 – B, BL3 – D
4	V004	SC - B, EC – B, blend B	BL1 – E, BL 2 – F, BL3 – G
5	V005	SC - A, EC – A, blend A	BL1 – A1, BL 2 – B, BL3 – H
6	V006	SC - A, EC – A, blend A	BL1 – A2, BL 2 – B, BL3 – H
7	V007	SC - A, EC – A, blend A	BL1 – A3, BL 2 – B1, BL3 – H
8	V008	SC - A, EC – A, blend A	BL1 – A4, BL 2 – B2, BL3 – H
9	V009	SC - A, EC – A, blend A	BL1 – I, BL 2 – J, BL3 – H
10	V011	SC - A, EC – A, blend A	BL1 – A2, BL 2 – B3, BL3 – H
11	V010	SC - B, EC – B, blend B	BL1 – A, BL 2 – B, BL3 – H
12	V012	SC - A, EC – A, blend A	Mass production
NOTE: SC – Steel Cord, EC – End Count, BL1, BL2, BL3 – individual Buffer Linings			

At first, the tire casings were tested using a non-destructive analyzer to see whether there are any hidden internal defects in the tire casing. After in-service for 20 hours that is about 800 km, the non-destructive analysis was carried out again and it was possible to see small local defects in the zone of the shoulder and bead. After each 800 km, the non-destructive analysis was carried out, and there was occurrence of visible small local defects. The given procedure was repeated until the casing was shut down by the touch sensor or until it was damaged. The individual defect zones were counted using a millimeter grid (planimetry). The grid-based counting method is not absolutely accurate but it is quite sufficient for our comparative purposes. There were 12 variants subjected to testing with non-destructive analyzer but for demonstration, images from only one variant are shown in this paper.

During the first testing, when the casing had not been subjected to any test yet, the defects were not detected in the casing with the non-destructive analyzer (Fig. 27). Subsequently, the given casing was further tested, using a 75 kN drum fatigue testing machine. After 20 hours, the first small local defects in the shoulders started to occur in the casing (Fig. 28).

After in-service of tire for further 20 hours (40 hours) or after 1,600 km, there was the occurrence of defects above the bead as well as small local defects in the shoulders and as it can be seen in the scans from the non-destructive analyzer, they even started to be joined gradually around the circumference (Fig. 29).

After 60 hours of tire in-service (cca 2,400 km), the defects started to be propagated noticeably in the casing. In the area above the bead, the individual local defects were joined together into the larger ones and moreover, at the same time, they were propagated towards the shoulders. In the shoulder, the defects were joined almost all the way around the whole circumference and they continued in their propagation to the crown (Fig. 30).

After the in-service of tire for 80 hours (cca 3,200 km), the test was stopped with the tire touch sensor shutting down due to a large defect above the bead. The defects above the bead had the increasing propagation character and they stared to join around the circumference. In the shoulder, they were propagated increasingly into the crown as well as into the sidewall of the casing (Fig. 31).

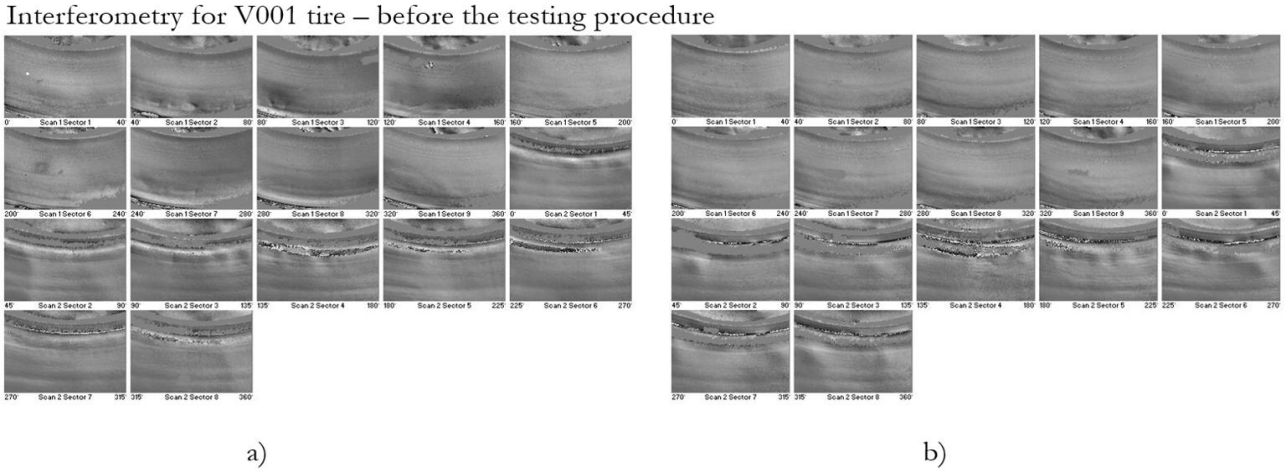

Fig. 27 *The first measurement of V001 tire – before the dynamic test, using the serial interferometric diagnostics; (a) Serial side (with DOT designation), (b) Non-serial side (without DOT designation)*

ISSN 1213–2489
e-ISSN 2787–9402

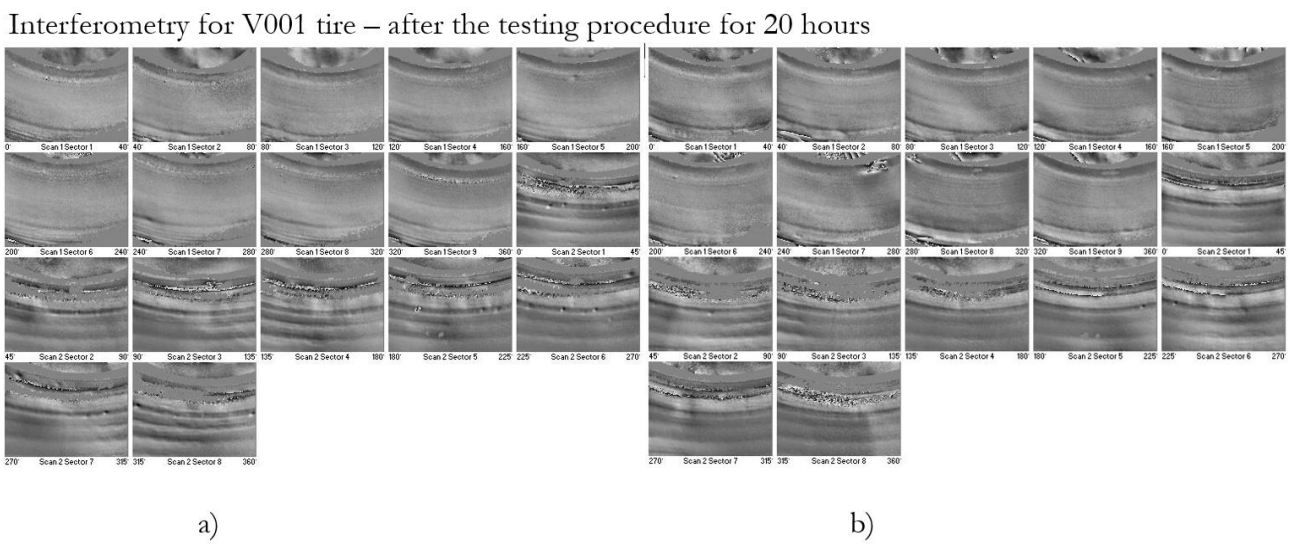

Fig. 28 *The second measurement of V001 tire after the in-service for 20 hours (cca 800 km), using the serial interferometric diagnostics; (a) Serial side (with DOT designation), (b) Non-serial side (without DOT designation)*

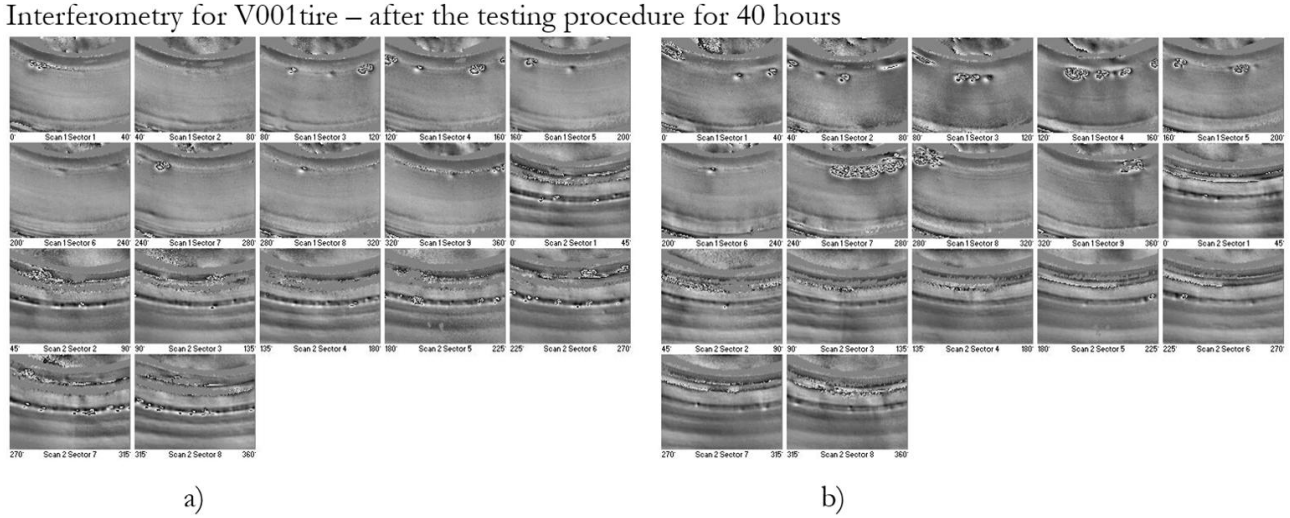

Fig. 29 *The third measurement of V001 tire after the in-service for 40 hours (cca 1,600 km), using the serial interferometric diagnostics; (a) Serial side (with DOT designation), (b) Non-serial side (without DOT designation)*

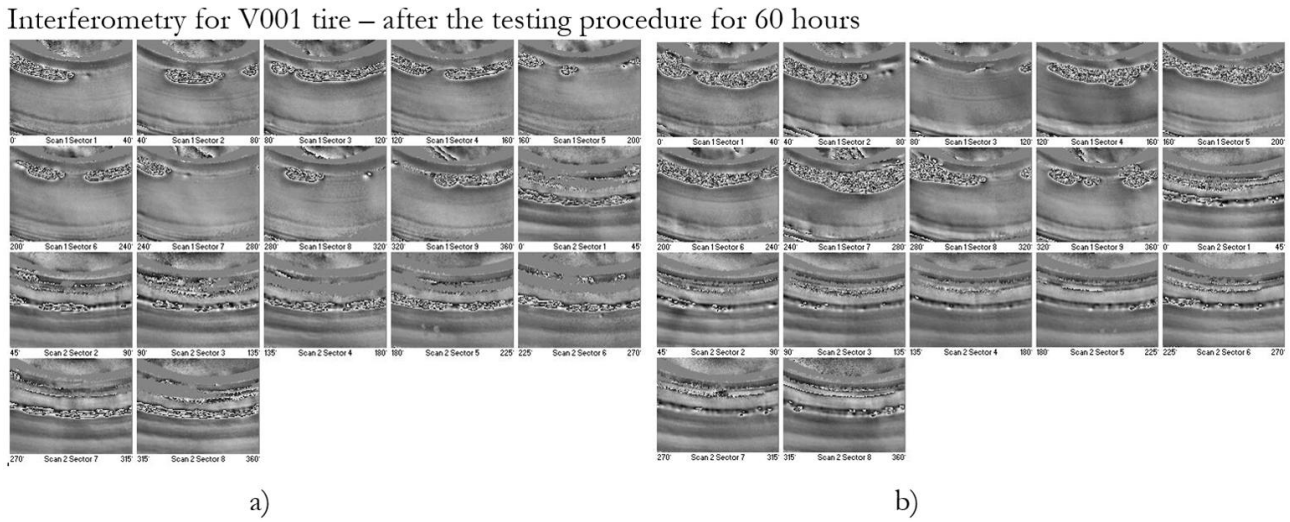

Fig. 30 *The fourth measurement of V001 tire after the in-service for 60 hours (cca 2,400 km), using the serial interferometric diagnostics; (a) Serial side (with DOT designation), (b) Non-serial side (without DOT designation)*

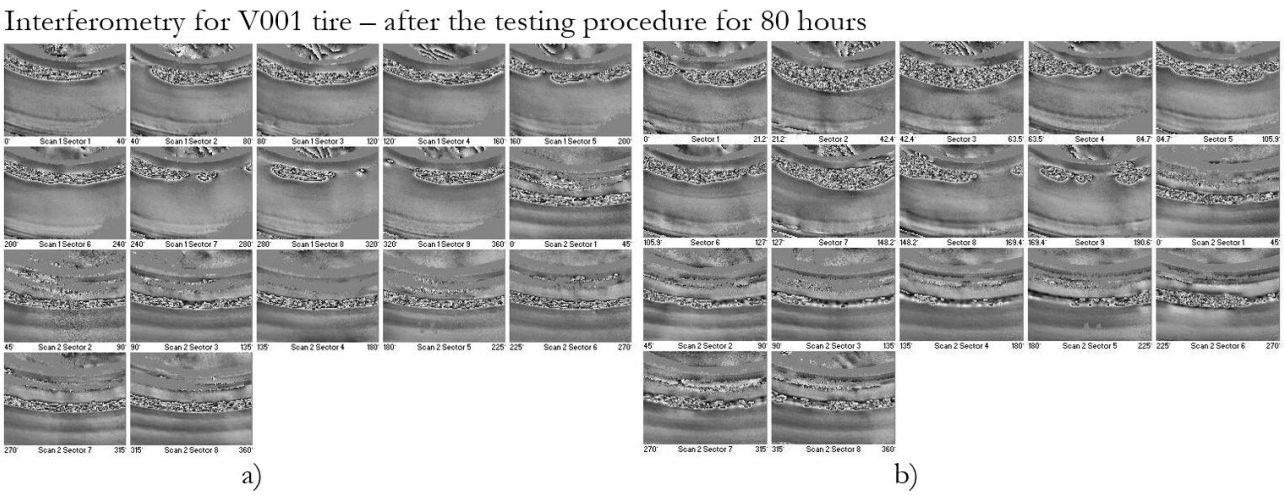

Fig. 31 *The fifth measurement of V001 tire after the in-service for 80 hours (cca 3,200 km), using the serial interferometric diagnostics – the end of the testing procedure; (a) Serial side (with DOT designation), (b) Non-serial side (without DOT designation)*

Before the performance of fatigue testing, the tire footprints on the pressure sensitive film were also made for each variant in order to observe the pressure distribution in the tire under the static loading. Fig. 32 shows the footprint before the dynamic test.

The tire loading was 14 225 N and inflation was 575 kPa. The average specific tire pressure was 353 kPa.

For the first two variants of tire (V001 and V002), the tire footprint on the pressure-sensitive film was carried out only before the test but for the other variants, the given footprint was also performed after in-service for 20 hours that corresponds to the in-service of tire for cca 800 km (Fig. 33).

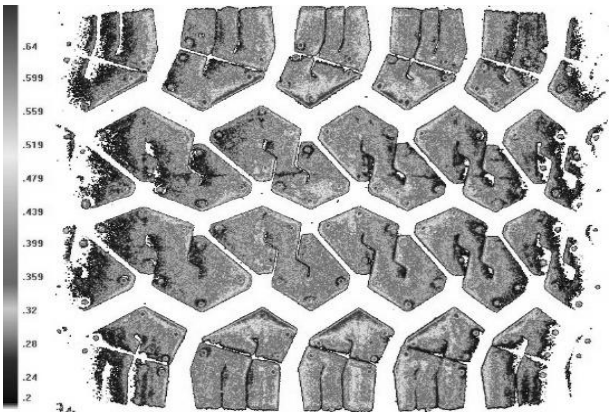

Fig. 32 *The tire footprint for V001 tire – before the dynamic test*

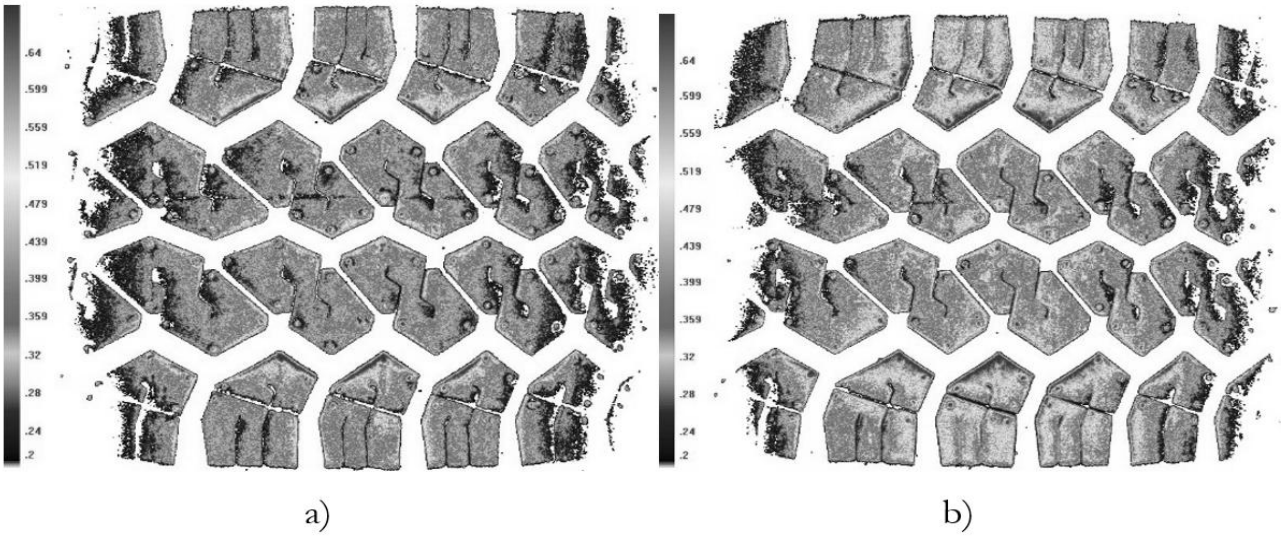

Fig. 33 *The tire footprint for V003 tire; a) before the dynamic testing, b) after 20 hours of dynamic testing*

The tire loading was 14 225 N and inflation was 575 kPa at average specific tire pressure. Before the testing, the average specific tire pressure for V003 was 343 kPa and after the in-service for 20 hours the average specific pressure was increased to 390 kPa.

As it can be seen from the pressure distribution in the tire footprint, the tires before the test exhibits the lower pressure in the crown and shoulder area and the highest pressure was in the area of the outermost tread profiles towards the crown of the tire. After in-service

for 800 km, the pressure distribution was changed. The pressure was increased at the crown area as well as at the area of the outermost tread profiles. This was the typical behavior for all tire variants except for V008 and V009, where the pressure was higher before the test than after the test. From this distribution of pressures, it can be assumed that shoulder defects can occur during in-service and that the highest wear can occur in the outermost tread profiles of the tire.

After completion of the test, cut sections were made for the defect areas where the given defects were detected with the non-destructive analyzer. From the individual cut sections can be determined that there are the defects in the shoulder and above the bead. The defects in the shoulder were initiated and propagated between the first and the second buffer lining in the site of their ending point. In the bead area, the defect was initiated above the bead bundle, between the carcass and the bead buffer linings (Fig. 34 and Fig. 37).

Tire cut sections for V001

Fig. 34 *The cut section of No. 1 casing – Scan 1, Sector 1 – serial side – the defect above the bead*

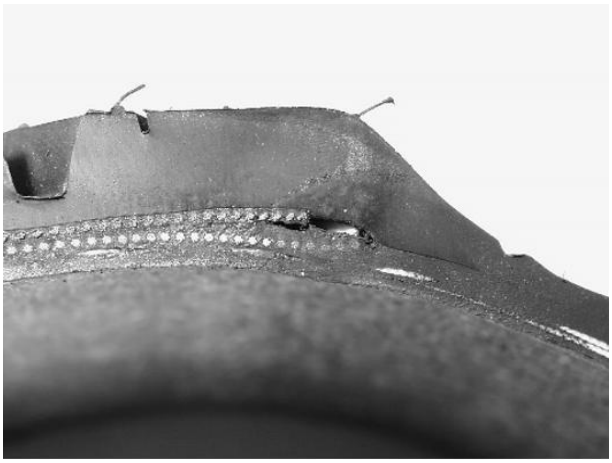

Fig. 35 *The cut section of No. 1 casing – Scan 2, Sector 2 – non-serial side – the defect in the shoulder between the buffer linings*

Fig. 36 *Cut section of No. 1 casing– Scan 1, Sector 6 – serial side – the defect above the bead*

Fig. 37 *Cut section of No. 1 casing – Scan 1, Sector 1 – non-serial side – the defect above the bead; The same testing procedure was used for all of the other variants of casings with the same dimensional proportions.*

In relation to the investigated variants, the Figures from 38 to 41 represent the graphs of the comparisons of the defects for the bead, shoulder and whole casing area after 40 hours (about 1,600 km). The comparison was made for 40 hours dynamic testing while the lowest performance was obtained with V004 and V010 and the highest performance was achieved with V011 and V012.

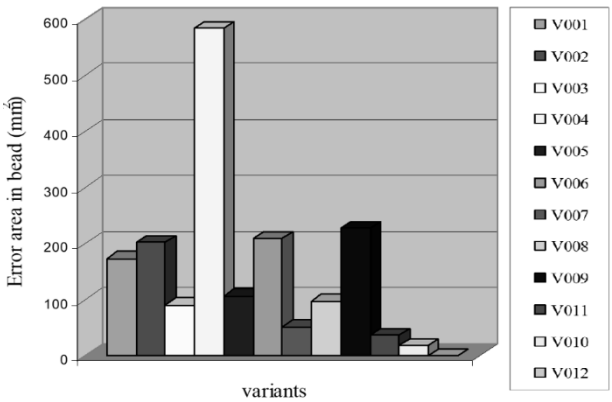

Fig. 38 *The representation of the defects zone at the area above the bead after in-service for 40 hours (cca 1,600 km), considering the each tire variant*

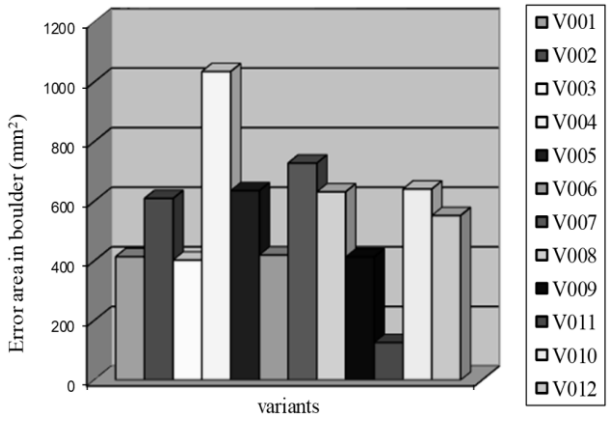

Fig. 39 *The representation of the defects zone at the area of the shoulder after in-service for 40 hours (cca 1,600 km) considering the each tire variant*

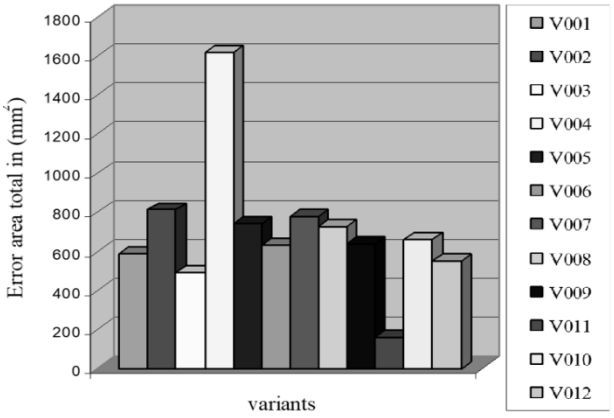

Fig. 40 *The representation of the defects zone for the tire as a whole after in-service for 40 hours (cca 1,600 km) considering the each tire variant*

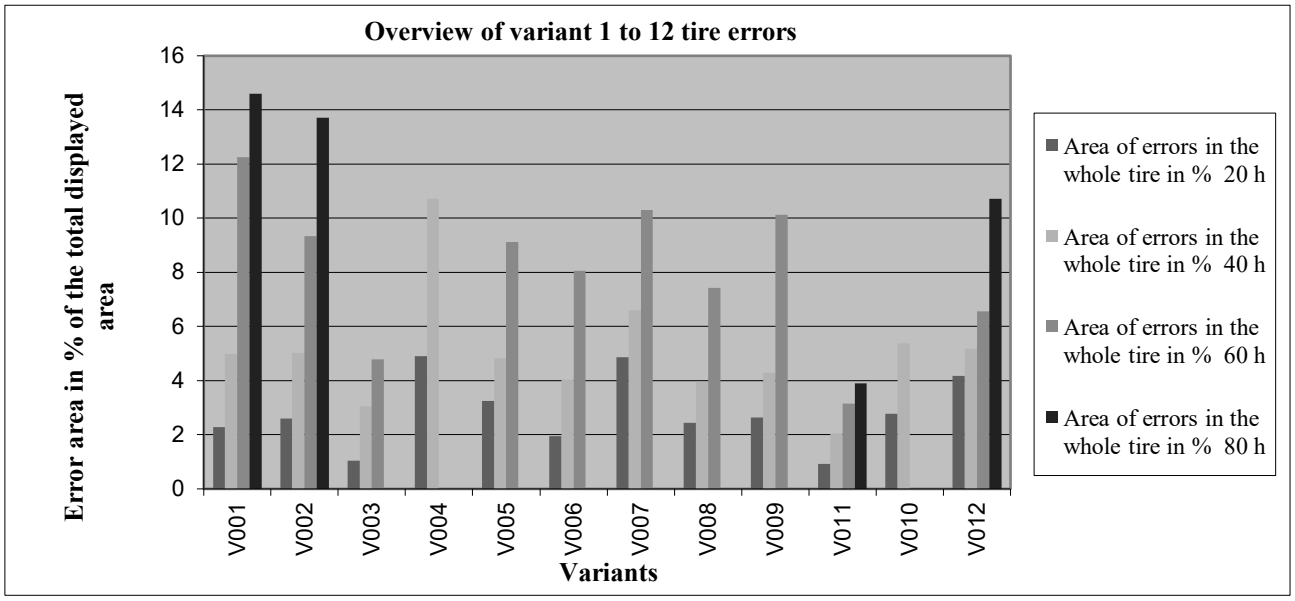

Fig. 41 *The comparison of the different tire variants after the in-service for 800 km, 1600 km, 2400 km, 3200 km and 4000 km, depending on the % of defects for the whole tire*

7 Discussion

It is necessary to point out that only after in-service of 1,600 km, there was the lowest performance exhibited in the case of casings with designation of No. 4 and No. 11 that is V004 and V010, respectively. These two casings, where the steel cord type and end count were designated as B, were made of B blend. The results show that the B-designated material is not suitable to be used for shoulder components where the high demands are closely connected with the dynamic properties of the tire. The A-designated material (see Table 1) was used for the production of the other tires. The performance of these tires ranged from 2 400 km to 4 000 km. This specification shows that the tire lifetime is influenced by the application of the suitable material as well as by the design or construction of the relevant tire parts (components) and tire areas. The highest performance and slowest propagation of defects was observed for No. 10 and No.12 casings, while the best performance, in terms of percentage of defects for the whole casing, was No. 10 casing (V011). The given tire casing (V011) was recommended by the development staff as the most suitable of the variants investigated. For bead area, the blend, used for production of No. 12 casing (V012), was recommended to be applied for casing production because of the occurrence of the smallest defects relating to the bead area.

Although it is a passive experiment, the contribution of this investigation is that it was not necessary to use high number of tested casings for each variant – only one piece of casing was needed to be used for dynamic testing because after each procedure (a certain number of in-service kilometers), the location of the defect, including its initiation and propagation, was accurately determined by non-destructive analysis, thus saving considerable financial resources.

Due to this investigation, the developing engineers obtained and brought the contributive overview in relation to the most suitable variant and at the same time, the important information on the zones and areas where there is the defect initiation as well as the way of their propagation. Based on this knowledge, critical areas of the casing can be more easily specified and a clear decision can be done in relation to selection of suitable variant to be used in production process.

8 Conclusions

The method of shearography (laser shearing interferometry) is applicable for the detection of defects in the field of laboratory testing, relating to automotive tire casings. Moreover it can be also used for the quality control of manufactured products. The advantage of this method is that there is not special preparation of the tire casings required and the testing process and analysis can be performed more times while the predetermined parameters are changed in dependence on desired resulting parameters.

The location of the defect, its initiation and propagation in specific tire areas can be determined accurately by non-destructive analysis after each step (procedure) of the dynamic test which is based on simulation of the in-service condition – in our case, it was the simulation, when the tire was in-service for a predetermined certain time interval or certain number of kilometers. By this way, described hereinbefore, it is possible to save considerable financial costs, compared with cutting the tire after each step for destructive analysis.

Based on the knowledge of defect initiation and propagation, the critical areas of the casing can be specified and controlled more easily and a clear decision can be done in relation to selection of suitable variant to be used in production process.

In this investigation, the assumption of rapid propagation of local defects in the shoulder and the sidewall areas and above the bead was verified. Moreover, the assumption that propagation of small local defects in the crown had slow rate or that there is even not any propagation was also confirmed. Based on this fact relating to the crown, the given tire casings, where the small local defects were or even were not determined with the non-destructive analysis, can be subjected to further dynamic testing because the mentioned small local defects will not significantly affect the further testing performance. In relation to shoulder and bead area, some of the tire casings have to be excluded from the investigation process because the small local defects can affect the testing performance in a negative way during dynamic testing and from the practical aspect, due to this defects, they are not allowed to be used in-service in order to avoid any accident, regarding road safety and protection of human life.

In comparison with the real conditions on the road, there are the slightly different conditions relating to the dynamic testing of tire, using the drum testing machines. It was interesting to observe the initiation and propagation of defects during the exploitative tests while the time interval or numbers of kilometers for tested tire in service were strictly predetermined. During the investigation of the defects the safety on the road and protection of the human lives was also taken into account.

In the future, it would be useful to extend the observation relating to the effect of tire inflation on the defect initiation and propagation, using the dynamic tests.

By studying the propagation of defects in this way, the developing engineers can enhance the overview relating to the most suitable variant and at the same time, the important information on the zones and areas with defect initiation and propagation where. Based on this information, the critical areas of the casing can be more easily recognized and the most suitable tire variant can be selected in order to be used in the process of production.

9 Addendum

The aim of this research was to determine the most suitable tire variant from V001 to V012. The slowest spreading defects were found in tire no. 10, designated variant V011. Thanks to this research, development engineers gained an overview of the most suitable variant, V011, as well as important information about the zones and areas where defects occur and how they spread. The occurrence and spread of defects is influenced not only by the material, but also to a large extent by the construction of the tire. This research involved a passive experiment, and its evaluation using statistical methods for 12 different variants is demanding not only in terms of time but also economically. Therefore, the research will continue with one tire variant, No. 10 variant V011, based on statistical analysis of five tires using an active factor experiment [23].

Acknowledgement

This work was supported by the Slovak Grant Agency – project KEGA 011TnUAD-4/2024.

References

[1] YEAGER, B. (2003). Non-destructive evaluation of radials. Tire Technology. In: *Internatinal – The Annual Review*, pp. 80-86

[2] YEAGER, R., W. (2004). Principles of shearography and its application in non-destructive testing Tire. Technology International, In: *UK& International Press*, pp.106-110

[3] BARRIERE, C., ROYER, D. (2001). Optical measurement of large transient mechanical . In: *Applied physics letters*. 8/2001, pp. 615-616

[4] DOEGE, E., SCHMIDT, R., JUNGERSEN, S., HUININK, J., YUN, W. (2003). Development of an optical sensor for the measurement of the material flow in deep drawing process. In: *Manufacturing technology 2003*, pp. 225-229

[5] LIAO, J., B., WU, M., H. (1999). A coordinate measuring maschine vision system. In: *Computer industrie*, 4/1999, pp. 329-339

[6] DEGRIECK, J., VERLEYSEN, P. (2002). Determination of impact parameters by optical measurement of the impactor displacement. In: *Experimental mechanics*. 9/2002, pp. 298-302

[7] TSAI, T., H., FAN, K., C., MOU, J., I. (2002). A variable-resolution optical profile measurement systém. In: *Measurement science & TECHNOLOGIE*. 2/2002, pp. 190-197

[8] MISTOU, S., KARAMA, O., DALVERNY, O., SIQUIER, J., M. (2003). 3D non – contact measurement of strain and displacement on transparent plastic films by stereo correlation. In: *Mechanique & Industries*, 11/2003

[9] SEO, Y., CHO, S., KANG, S., N. (2003). Measurement of microthermal deformation in an optical pick up base using holographic interferometry. In: *Optical ingeneering*. 11/2003, pp. 3198-3214

[10] LI, X. (2003). Comparisons between instantaneus and integral intensities in dynamic speckle pattern interferometry. In: *Optics laser technologie*, 4/2003, pp. 203-223

[11] PHILLIPS, P. (1999). CCD camera as a microscop. In: *A standard cable and the benefits of new technologie*. 12/1999

[12] CABRERA, J., A. (2003). Versatile flat track tire testing maschine. In: *Vehicle system dynamics*, 10/2003, pp. 271-285

[13] SYMENS, R. (2003). Sidewall bulge and depression testing. In: *Tire technology International – The Annual Review*, pp. 112-114

[14] MARCÍN, J., ZÍTEK, P. (1985). *Rubber productions I – Tyres*. SNTL, Prague

[15] ONDRUŠOVÁ, D., PAJTÁŠOVÁ, M. (2011). *Rubber components and their influence on rubber properties and enviromental aspects of production*, pp. 166. Spolok Slovákov v Poľsku, Krakow. ISBN 978-83-7490-385-1

[16] VAVRO, J., HAJSKÁ, H., VAVRO, J. JR., VAVROVÁ, A. (2011). *Nové metódy a prístupy experimentálnej mechaniky pri identifikácií vád a porúch výrobkov*, pp. 265. Spolok Slovákov v Poľsku, Krakow. ISBN 978-83-7490-461-2

[17] VAVRO, J., VAVRO, J., JR. (2019). *Aplikácia výpočtových a experimentálnych metód v gumárenskom priemysle*, pp. 120. ASSA spol. s. r. o., Púchov. ISBN 978-80-8075-887-5

[18] SVOBODA, M., CHALUPA, M., ČERNOHLÁVEK, V., ŠVÁSTA, A., MELLER, A., SCHMID, V. (2023). Measuring the Quality of Driving Characteristics of a Passenger Car with Passive Shock Absorbers. In: *Manufacturing Technology*. Vol. 23, No. 1 ISSN 1213–2489 e-ISSN 2787–9402, DOI: 10.21062/mft.2023.023 © 2023

[19] VAŠINA, M., PÖSCHL, M., ZÁDRAPA, P. (2021). Influence of Rubber Composition on Mechanical Properties. In: *Manufacturing Technology*. Vol. 21, No. 2 ISSN 1213–2489, DOI: 10.21062/mft.2021.021 © 2021

[20] VAŠINA, M., PÖSCHL, M., ZÁDRAPA, P. (2018). A Study of Significant Factors Affecting Viscoelastic Damping Properties of Polymer Materials. In: *Manufacturing Technology*. Vol. 18, No. 3: 523-529 | DOI: 10.21062/ujep/132.2018/a/1213-2489/MT/18/3/523

[21] BAKOŠOVÁ, D., BAKOŠOVÁ, A., DUBCOVÁ, P., KOŠTIALIKOVÁ, D., DUBEC, A., JANEKOVÁ, M. (2024). Effect of Filler Content and Treatment on Mechanical Properties of Polyamide Composites Reinforced with Short Carbon Fibres Grafted with Nano-SiO_2. In: *Manufacturing Technology*. Vol. 24, No. 4 ISSN 1213–2489 e-ISSN 2787–9402, DOI: 10.21062/mft.2024.058 © 2024

[22] BAKOŠOVÁ, D. (2018). Dynamic Mechanical Analysis of Rubber Mixtures filled by Carbon Nanotubes. In: *Manufacturing Technology*. Vol. 18, No. 3 ISSN 1213–2489, DOI: 10.21062/ujep/103.2018/a/1213-2489/MT/18/3/345

[23] VAVRO, J., VAVRO, J., JR., VAVROVÁ, A., SUCHÁ, D. (2009). Faktorový experiment šírenia sa separácie v plášti pneumatiky osobného vozidla. In: *7th International conference, Dynamics of rigid and deformable bodies 2009,* pp. 179-184. Ústí and Labem, Czech republic, ISBN 978-80-7414-153-9